

3D FINITE ELEMENT SIMULATION OF POLYMER EXTRUDATE IN FDM 3D PRINTERS

Sim-AM 2019

ONUR HIRA* AND ATAKAN ALTINKAYNAK*

* Mechanical Engineering Department
Istanbul Technical University
Gumussuyu Campus, 34437 Istanbul, Turkey
e-mail: altinkayna@itu.edu.tr, web page: <http://akademi.itu.edu.tr/altinkayna/>

Key words: Fused Deposition Modelling (FDM), Polymer Extrudate Shape, Finite Element Method, Level Set Method

Abstract. 3D finite element simulation of a FDM printer nozzle region was performed using COMSOL Multiphysics software. The polymer exiting the nozzle of the FDM printer was also included in the simulation in order to capture the dimensional behavior of the polymer. The domain of the simulation consisted of a nozzle, printer table, and the surrounding air. In the simulation, mass and momentum equations were solved to determine the non-Newtonian flow characteristics of the polymer. The interface between the polymer and ambient air was modelled using the level set method. Experiments were conducted to validate the numerical results. One experimental specimen with 30 strips was printed using a 3D printer. In the CAD model of the specimen, each strip had the same width as the nozzle diameter. While printing, it was ensured that the nozzle had only one continuous vertical movement to print each strip. The printed strips were measured with a caliper at five different locations. The difference between the numerical and experimental results of strip width were less than 10%. The developed model provided information about the transient shape of the polymer extrudate and can be used to predict the dimensional accuracy of the FDM-printed parts.

1 INTRODUCTION

Additive manufacturing methods, also known as 3D printing, have the advantage of manufacturing complex geometries [1]. Out of various types of additive manufacturing techniques, Fused Deposition Modelling (FDM) is perhaps the most popular when low-cost is important [2]. In FDM, a structure is built layer by layer by discharging a stream of material from a nozzle. Even though thermoplastics have been commonly used for FDM process [3], other materials such as fiber-reinforced polymers [4], bio-degradable materials [5], ceramic [6], and concrete [7] are also available.

FDM is a rapidly progressing branch of additive manufacturing. Researchers have conducted several experimental studies to improve the process of FDM and part quality [8]. The investigated parameters have generally been layer thickness and orientation, infill type and rate, extrusion angle, and nozzle diameter [9]. The quality of FDM parts also depends on extrusion temperature and feed rate [10]. These parameters have an effect on residual stresses, shrinkage and bonding quality [11-13]. Due to the vast number of process parameters, many studies have been focused on finding optimal settings for manufacturing time, surface quality,

dimensional tolerances, and mechanical strength [1, 14-16].

In recent years, researchers have paid more attention to the numerical simulations of FDM process. Initial attempts were focused on the thermomechanical simulations of the final part in order to determine the characteristics of shrinkage, warpage, residual stresses, and potential crack initiation locations [17-19]. Current numerical studies are based on three dimensional CFD simulations. Non-isothermal and non-Newtonian flow, cooling, and solidification of polymer were simulated in a FDM process [20, 21]. Viscoelastic stresses were included in the model later [22]. An isothermal and Newtonian model was developed to simulate the deposition of polymer on a moving plane [23] and the model was validated with experiments [24]. It was found that the shape of extrudate changed from circle to rectangle as the gap height to velocity ratio decreased. Successive deposition of extrudate layer simulations showed that the layer thickness and distance between extrudates influenced the previous extrudate shape and pore formation [25]. In these numerical models, polymer was assumed to be discharged from a cylindrical volume.

In this work, the nozzle region of a FDM printer was simulated using finite element method. The simulations included the nozzle with a flow channel, printer table, and the air surrounding the nozzle region. Level set method was used to predict the shape of the polymer discharged from the nozzle. The polymer/printer table contact was also considered in the simulations. Non-Newtonian characteristics of the polymer was taken into account for predictions. An experimental sample was printed to validate the numerical simulations.

2 EXPERIMENTAL METHOD

ABS filament was used to perform experiments at nozzle temperature of 220°C and feed rate of 40 mm/s. Two rows and 15 columns of strips with dimensions of 0.4 mm width and height were printed on a 0.1 mm thick base. The dimensions of the printed sample are shown in Fig. 1.

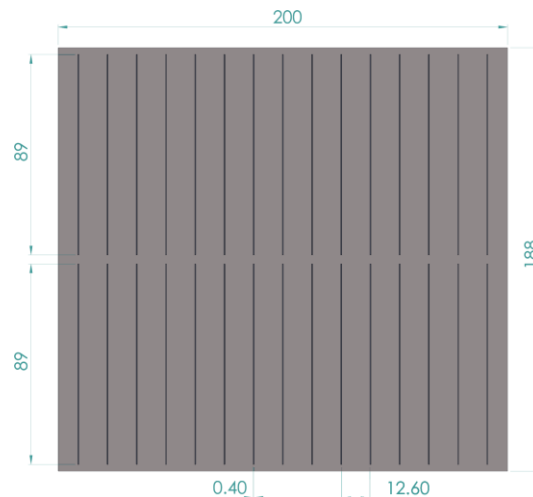


Figure 1: A schematic of the sample with dimensions

The diameter of the nozzle was 0.4 mm which was the same as the strip width on CAD data supplied to the slicer software. One continuous vertical movement of the nozzle was

enforced to print each strip. Experiment was performed at a printer temperature of 80°C. Each strip was measured at five positions to compare the experimental data with the numerical results.

3 NUMERICAL METHOD

The discharge and the deposition of ABS polymer on printer table were simulated using COMSOL Multiphysics 5.4 software. The cross-section of the 3D domain is shown in Fig. 2. The domain included the flow channel, nozzle, printer table, and the surrounding air. The molten polymer entered the flow channel from the inlet. The nozzle tip was located 0.2 mm above the printer table. This value was the same as the layer thickness in the experiment. The flow was defined as fully developed at the inlet, and the average velocity was calculated based on the experimental feed rate of 40 mm/s. The average velocity at the entrance was increased from zero to steady-state in one second. The printer table velocity in the vicinity of polymer deposition was set to feed rate speed in order to convey the extruded polymer towards the outlet. No slip condition was enforced on the nozzle/polymer boundaries. The simulation was performed for a period of time taken to print one strip.

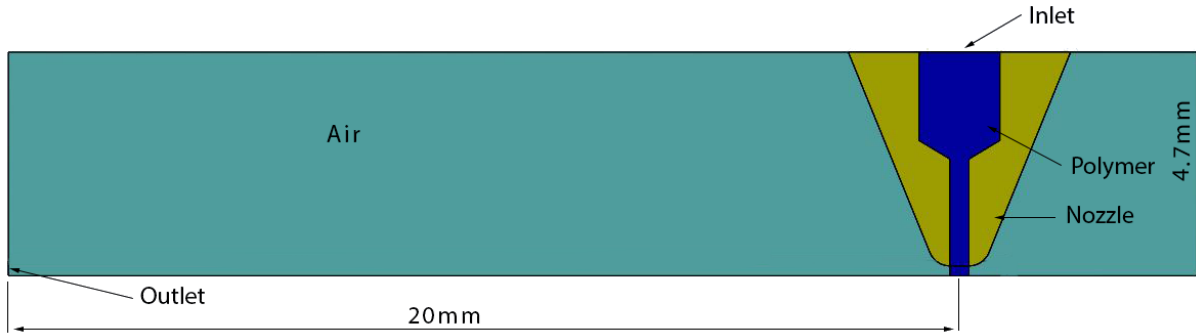


Figure 2: The cross-section of the 3D domain

The continuity and momentum equations were solved to simulate the polymer flow and deposition. The effect of temperature was not taken into account in this study. The shear rate dependence of polymer shear viscosity was modelled using Cross [26] model (Eq. 1).

$$\eta_s = \frac{\eta_0}{1 + \left(\frac{\eta_0 \dot{\gamma}}{\tau^*} \right)^{1-n}} \quad (1)$$

where η_0 is the zero-shear viscosity, $\dot{\gamma}$ is the shear rate, and τ^* and n are material-dependent constants. These material constants and material properties such as density, heat capacity, and thermal conductivity were obtained from the literature [27] and are presented in Table 1.

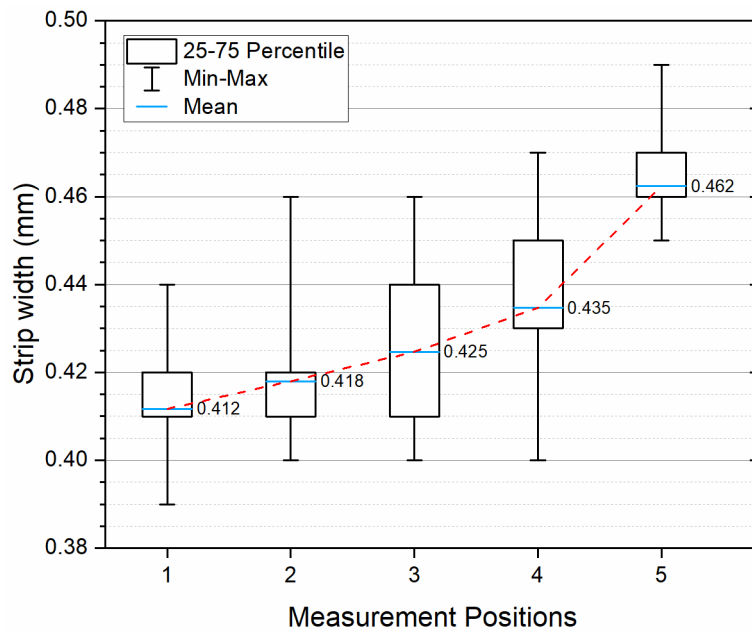
Besides solving the continuity and momentum equations, one transport equation was also solved to determine the interface between the polymer and ambient air using level set method. In level set method, level set function (ϕ) represents the interface between two domains. The value of ϕ varies from zero to one indicating the transition from one domain to the other. In this study, $\phi = 0.5$ was used to define the polymer/air interface.

Table 1: Material parameters used in the numerical simulation

	Density (gr/cm ³)	Heat Capacity (J/(kg K))	Thermal Conductivity (W/(m K))	τ^* (Pa)	n
ABS	1040	2345	0.18	2.90×10^4	0.33

4 RESULTS AND DISCUSSIONS

The experimental measurements obtained from the ABS sample printed at 40 mm/s are shown in Fig. 3. The average of measured strip width at five locations varied between 0.41 and 0.46 mm. The overall average of strip width was calculated as 0.430 mm indicating a difference of 7.5% compared to the nominal width of 0.4 mm. Figure 3 shows that the measured width had the tendency to increase along the printing direction. This characteristic may be due to the control algorithm of the nozzle and feed rate. Prior to printing, the polymer and the nozzle are generally at rest. While the nozzle accelerates to the steady state velocity, the filament is also pushed into the nozzle to supply the required material. The control of these two parameters will affect the amount of material discharged from the nozzle per unit time.

**Figure 3:** Measured strip width of ABS sample at five separate positions along the strip

The simulation result of polymer flow and deposition on printer table at 40 mm/s is presented in Fig. 4. The deposited ABS was conveyed along the z -axis. The extrudate shape away from the nozzle exit was dome-like. However, a barrel-like shape was observed near the nozzle exit. Previous experimental and numerical study suggested a barrel-like cross-section when the layer height is relatively small [24]. It is also evident that some of the polymer escalated on the nozzle surface facing towards the deposited material. The amount of polymer elevation is shown in Fig. 5 ($z=0.5$). The cross-section of polymer/air interface started as a

rectangular shape at the discharge and converted into a dome shape right after. The height of the strip increased above 0.3 mm and then decreased as low as 0.1 mm. The linear decrease of strip height beyond $z=2$ mm was expected and it was due to the transient increase of feed rate during the first 1 s.

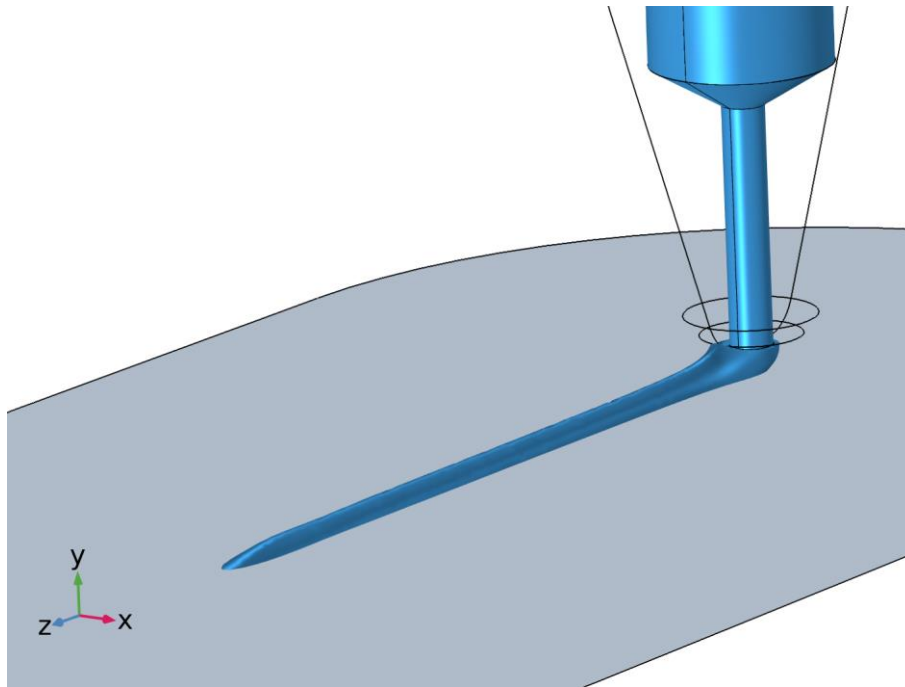


Figure 4: Predicted ABS deposition on printer table at 40 mm/s during 0.7 s.

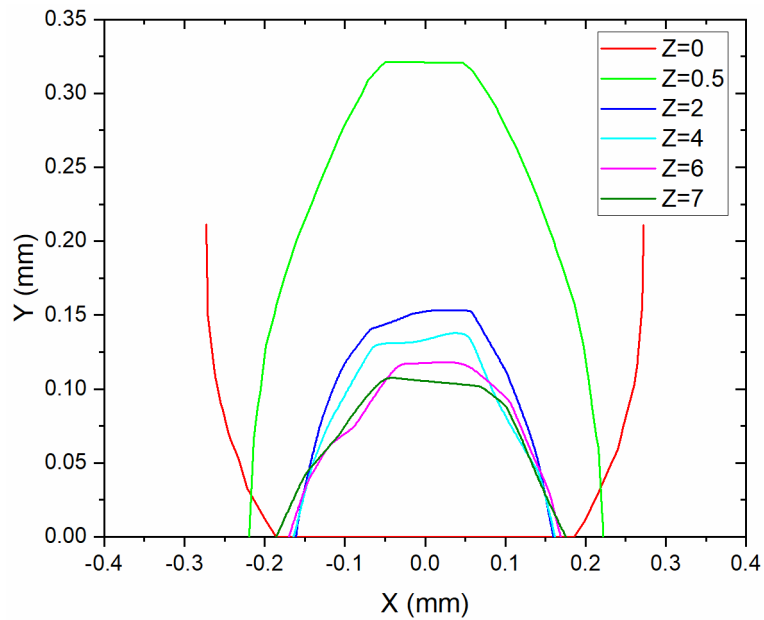


Figure 5: The cross-section of polymer/air interface along the printing direction at 0.7 s.

The mean strip width from the numerical simulations was 0.371 mm which was moderately lower than the experimental result of 0.430 mm. Once the steady state was reached after a period of 1 s, the strip width was essentially the same at measurement locations. Even though 0.441 mm strip width was obtained at a distance of $z=0.5$ mm, both the strip width and height were instantly decreased to lower values at $z=2$ mm. The reason for this shape change may be due to the lack of temperature dependency of shear viscosity. Shear viscosity of polymers decreases drastically with temperature especially when the temperature is below the glass transition temperature. The experimental printer temperature was 80°C which was lower than the glass transition temperature of ABS. Once the non-isothermal simulations are performed, the polymer touching the printer table is expected to have much higher shear viscosity which will limit the deformation of the polymer.

5 CONCLUSIONS

- Three-dimensional finite element simulations of polymer flow and deposition on printer table were performed. The simulations included the non-Newtonian characteristics of the polymer shear viscosity. The polymer/air interface was determined using the level set method. Experimental sample was printed to validate the numerical model.
- The shape of the strip changed from rectangular shape to dome shape right after the nozzle tip. The numerical result was 13.7% lower than that of the experimental result. Non-isothermal effects were not included in the model. Particularly, updating the model with temperature dependency of the shear viscosity is expected to improve the predictions.
- The developed numerical model can be used to understand the relationship between process parameters and the dimensional accuracy of FDM-printed parts. Further improvements can be implemented to reduce the discrepancies between the experimental and numerical results.

6 ACKNOWLEDGMENTS

This work was supported by TÜBİTAK Project No: 217M687.

REFERENCES

- [1] Turner, B.N. and S.A. Gold, *A review of melt extrusion additive manufacturing processes: II. Materials, dimensional accuracy, and surface roughness*. Rapid Prototyping Journal, 2015. **21**(3): 250-261.
- [2] N. Turner, B., R. Strong, and S. A. Gold, *A review of melt extrusion additive manufacturing processes: I. Process design and modeling*. Rapid Prototyping Journal, 2014. **20**(3): 192-204.
- [3] Cicek, O.Y., A. Altinkaynak, and E.C. Balta. *Numerical and experimental analysis of infill rate on the mechanical properties of fused deposition modelling polylactic acid parts*. in *Proceedings of the SPE ANTEC®*. 2017. Anaheim, CA, USA: 75-81.
- [4] Zhong, W., F. Li, Z. Zhang, L. Song, and Z. Li, *Short fiber reinforced composites for fused deposition modeling*. Materials Science and Engineering: A, 2001. **301**(2): 125-130.

- [5] Zein, I., D.W. Hutmacher, K.C. Tan, and S.H. Teoh, *Fused deposition modeling of novel scaffold architectures for tissue engineering applications*. *Biomaterials*, 2002. **23**(4): 1169-1185.
- [6] Bellini, A., *Fused deposition of ceramics: a comprehensive experimental, analytical and computational study of material behavior, fabrication process and equipment design*. 2002, Drexel University, Ann Arbor, MI.
- [7] Gosselin, C., R. Duballet, P. Roux, N. Gaudillière, J. Dirrenberger, and P. Morel, *Large-scale 3D printing of ultra-high performance concrete—a new processing route for architects and builders*. *Materials & Design*, 2016. **100**: 102-109.
- [8] Ngo, T.D., A. Kashani, G. Imbalzano, K.T. Nguyen, and D. Hui, *Additive manufacturing (3D printing): A review of materials, methods, applications and challenges*. *Composites Part B: Engineering*, 2018. **143**: 172-196.
- [9] Domingo-Espin, M., J.M. Puigoriol-Forcada, A.-A. Garcia-Granada, J. Llumà, S. Borros, and G. Reyes, *Mechanical property characterization and simulation of fused deposition modeling Polycarbonate parts*. *Materials & Design*, 2015. **83**: 670-677.
- [10] Kaveh, M., M. Badrossamay, E. Foroozmehr, and A.H. Etefagh, *Optimization of the printing parameters affecting dimensional accuracy and internal cavity for HIPS material used in fused deposition modeling processes*. *Journal of Materials processing technology*, 2015. **226**: 280-286.
- [11] Alhubail, M., *Statistical-based optimization of process parameters of fused deposition modelling for improved quality*. 2012, University of Portsmouth.
- [12] Monzón, M.D., I. Gibson, A.N. Benítez, L. Lorenzo, P.M. Hernandez, and M.D. Marrero, *Process and material behavior modeling for a new design of micro-additive fused deposition*. *The International Journal of Advanced Manufacturing Technology*, 2013. **67**(9-12): 2717-2726.
- [13] Costa, S., F. Duarte, and J. Covas, *Estimation of filament temperature and adhesion development in fused deposition techniques*. *Journal of Materials Processing Technology*, 2017. **245**: 167-179.
- [14] Mohan, N., P. Senthil, S. Vinodh, and N. Jayanth, *A review on composite materials and process parameters optimisation for the fused deposition modelling process*. *Virtual and Physical Prototyping*, 2017. **12**(1): 47-59.
- [15] Mohamed, O.A., S.H. Masood, and J.L. Bhowmik, *Optimization of fused deposition modeling process parameters: a review of current research and future prospects*. *Advances in Manufacturing*, 2015. **3**(1): 42-53.
- [16] Li, H., T. Wang, and Z. Yu, *The quantitative research of interaction between key parameters and the effects on mechanical property in FDM*. *Advances in Materials Science and Engineering*, 2017. **2017**.
- [17] Brenken, B., E. Barocio, A. Favaloro, and R.B. Pipes, *Simulation of semi-crystalline composites in the extrusion deposition additive manufacturing process*. *Science in the Age of Experience*, 2017: 90-102.
- [18] Talagani, M., S. DorMohammadi, R. Dutton, C. Godines, H. Baid, F. Abdi, V. Kunc, B. Compton, S. Simunovic, and C. Duty, *Numerical simulation of big area additive manufacturing (3D printing) of a full size car*. *SAMPE Journal*, 2015. **51**(4): 27-36.

- [19] Bikas, H., P. Stavropoulos, and G. Chryssolouris, *Additive manufacturing methods and modelling approaches: a critical review*. The International Journal of Advanced Manufacturing Technology, 2016. **83**(1-4): 389-405.
- [20] Xia, H., J. Lu, S. Dabiri, and G. Tryggvason, *Fully resolved numerical simulations of fused deposition modeling. Part I: fluid flow*. Rapid Prototyping Journal, 2018. **24**(2): 463-476.
- [21] Xia, H., J. Lu, and G. Tryggvason, *Fully resolved numerical simulations of fused deposition modeling. Part II—solidification, residual stresses and modeling of the nozzle*. Rapid Prototyping Journal, 2018. **24**(6): 973-987.
- [22] Xia, H., J. Lu, and G. Tryggvason, *A numerical study of the effect of viscoelastic stresses in fused filament fabrication*. Computer Methods in Applied Mechanics and Engineering, 2019. **346**: 242-259.
- [23] Comminal, R., M.P. Serdeczny, D.B. Pedersen, and J. Spangenberg, *Numerical modeling of the strand deposition flow in extrusion-based additive manufacturing*. Additive Manufacturing, 2018. **20**: 68-76.
- [24] Serdeczny, M.P., R. Comminal, D.B. Pedersen, and J. Spangenberg, *Experimental validation of a numerical model for the strand shape in material extrusion additive manufacturing*. Additive Manufacturing, 2018. **24**: 145-153.
- [25] Serdeczny, M.P., R. Comminal, D.B. Pedersen, and J. Spangenberg, *Numerical simulations of the mesostructure formation in material extrusion additive manufacturing*. Additive Manufacturing, 2019.
- [26] Cross, M.M., *Relation between viscoelasticity and shear-thinning behaviour in liquids*. Rheologica Acta, 1979. **18**(5): 609-614.
- [27] Altinkaynak, A., M. Gupta, M.A. Spalding, and S.L. Crabtree, *Melting in a Single Screw Extruder: Experiments and 3D Finite Element Simulations*. International Polymer Processing, 2011. **26**(2): 182-196.